Digital Discovery of interferometric Gravitational Wave Detectors

Anonymous Author(s)
Affiliation
Address
email

Abstract

Gravitational waves, detected a century after they were first theorized, are space-time distortions caused by some of the most cataclysmic events in the universe, including black hole mergers and supernovae. The successful detection of these waves has been made possible by ingenious detectors designed by human experts. Beyond these successful designs, the vast space of experimental configurations remains largely unexplored, offering an exciting territory potentially rich in innovative and unconventional detection strategies. Here, we demonstrate an intelligent computational strategy to explore this enormous space, discovering unorthodox topologies for gravitational wave (GW) detectors that significantly outperform the currently best-known designs under realistic experimental constraints. This increases the potentially observable volume of the universe by up to 50-fold. Moreover, by analysing the best solutions from our super-human algorithm, we uncover entirely new physics ideas at their core. At a bigger picture, our methodology can readily be extended to AI-driven design of experiments across wide domains of fundamental physics, opening fascinating new windows into the universe.

1 Introduction

Gravitational waves are ripples in space-time produced by enormous energetic astrophysical phenomena such as the collision of two black holes or supernovae. While predicted in 1916 by Einstein as a consequence of his General Relativity [1], they have only been directly observed 100 years later [2]. This discovery has opened a new window for the observation of phenomena in the universe, independent from electromagnetic waves, neutrinos or massive particle – and allowing for a new branch of multi-messenger astrophysics [3].

The current generation of GW detectors, the Advanced Laser Interferometer Gravitational-Wave Observatory (aLIGO) [4], exploit optical interferometry, which is sensitive to the distortion of space-time. The design is based on a Michelson interferometer with multi kilometer long arms, augmented with recycling cavities and squeezed vacuum sources for reducing various noise sources. LIGO's topology and design sensitivities of current and near-future upgrades are presented in Fig. 1A. These detectors have all been designed by human researchers following human design principles, sometimes augmented with small-scale computational optimization of detector parameters (such as finding the ideal laser power and mirrors' reflectivities and phases) [5, 6].

In this manuscript, we explore the vast space of potential new topologies for GW detectors using advanced large-scale computational exploration techniques. We rephrase the discrete (and thus computationally difficult) question of topology discovery into a tractable continuous optimization problem of a *universal interferometer* (UIFO) for GW detectors. We then focus on four GW frequency regimes motivated by exciting astrophysical phenomena, including black hole and neutron star mergers, supernovae, and primordial gravitational objects. In all frequency regimes, we discover

Submitted to 38th Conference on Neural Information Processing Systems (NeurIPS 2024). Do not distribute.

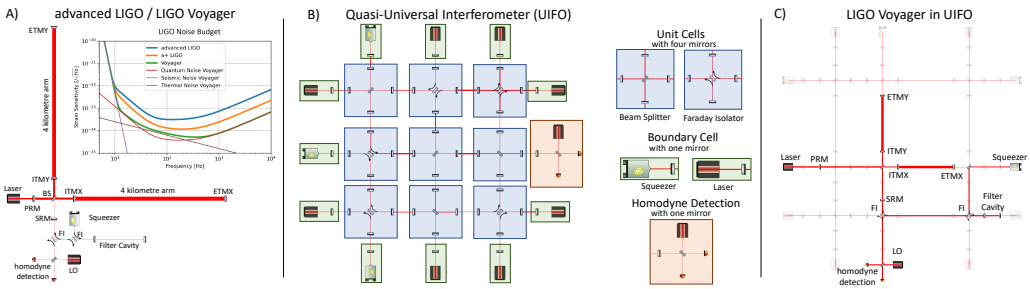

Figure 1: **Details of the current LIGO detectors and quasi-universal interferometer (UIFO)** A) Setup of LIGO's GW Detector: A Michelson interferometer with power-recycling mirrors and a filter cavity. Inset: The noise budget for generations of LIGO detectors: Advanced LIGO [7], A+ LIGO [8] and the next-generation Voyager detector [9]. B) A UIFO is a highly expressive parameterized template for an interferometer. It consists of $(n \times n)$ unit cells, light inputs at three of the four boundaries (left, up, and down). A unit cell consists of a beamsplitter or a 4-port Faraday isolator (FI) enclosed by four mirrors. The input light comes from a laser or a squeezed vacuum source. A detection scheme finally retrieves the signal. The individual elements are parametrized: Laser (power and relative phase), Squeezer (squeezing level and squeezing angle), mirror (transmission rate, relative phase, mass), beamsplitter (transmission rate, relative phase), and space (length). This ansatz has up to 187 parameters. C) One way to inscribe LIGO's next-generation detector into UIFO.

new GW topologies that outperform the current next-generation designs, under realistic experimental constraints, some of which are candidates for near-term upgrades. For several designs, we conceptualize the underlying physical principles and core functionalities. Our method can not only find new superior detection schemes for rare astrophysical events, but could also be used for designing gravitational-wave-based detectors for dark matter [10, 11], or aspects of quantum gravity [12, 13]. Our work shows how advanced computational design methods can inspire new unorthodox ideas for fundamental physics experiments. Taking a broader view – beyond parameter optimization – we see that there is an unimaginably large number of experimental topologies that have never been explored by human researchers. This suggests an enormous range of unexplored GW detector configurations that could not only surpass current leading designs but could also provide entirely new experimental concepts and ideas [14, 15, 16].

Digital Discovery Approach: *The enormous topological search space* – With only one laser, ten optical elements (mirrors or beamsplitters), and two detectors, we can already build more than 100 million unique configurations (see Appendix). Furthermore, each of these configurations has a large continuous search space spanned by the continuous parameters of the optical elements. This space contains many GW detector designs invented by human researchers, including aLIGO and next-generation detectors and many potential GW detectors that have not yet been discovered. Finding new GW detectors thus is a search problem in an extremely high-dimensional space.

Representing Gravitational Wave Detectors in a universal interferometer – We reformulate the mainly discrete search problem into a purely continuous optimization problem, by inventing a quasi-universal interferometer (UIFO), see Fig. 1B. The UIFO, which is inspired by the idea of universal function approximation of neural networks[17], is a highly expressive, parametrized optical interferometer. It consists of cells of beamsplitters (BS) enclosed by mirrors, and seeded by lasers or squeezers. A detector then finally retrieves the signal. The physical properties of the optical elements (such as laser power, phases, transmissivity of mirrors and beamsplitters), and the distances between them, are free parameters. The UIFO is constructed in such a way that setting the right parameters leads to different topological structures, e.g. we can encode the next-generation detector in Fig. 1C.

Astrophysical design targets – We search for new GW detectors with superior sensitivity in the frequency range of interesting astrophysical targets. Hence, we have to find precise parameter settings of the UIFO that lead to high sensitivity within the desired frequency range. We search for a broadband detector in the range of 20 – 5000 Hz for detections of universal sources such as binary black hole mergers, which coincides with the objective of aLIGO and the next-generation Voyager detector [4, 9]. Another target is high-sensitivity designs at low-frequency in the range of 10 – 30 Hz, which is the expected signal range of black hole mergers originating from the earliest stars in the

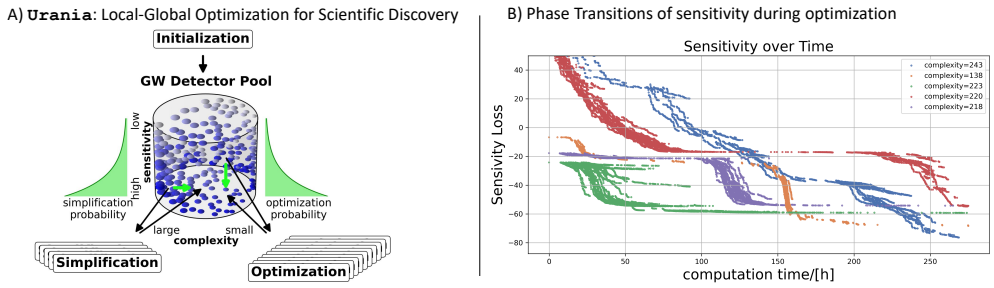

Figure 2: **Discovery engine `Urania` and optimisation phase transitions**: A) A pool of GW detectors is filled with random initialization of UIFOs (see Fig. 1 for details). The horizontal location of the dots stands for complexity, and the vertical for sensitivity. A large number of parallel independent optimization instances choose Boltzmann-distributed from the pool and locally optimize using numerical minimization of a loss function. Subsequently, and in parallel, automated pruning algorithms choose again Boltzmann-distributed from the pool and try to reduce the complexity of the solutions. B) Surprisingly, the optimization leads to phase transitions in loss curves. The evolution of the loss goes through long barren plateaus, followed by short periods where the loss decreases significantly where new physical abilities are discovered and exploited in a short period of time.

universe [18]. These early and distant black holes could be an interesting source of *dark sirens*, for precision measurement of the Hubble constant [19]. We also search for detectors for supernovæ explosions, which are expected in the range of 200 – 1000 Hz [20]. These signals have never been observed [21, 22, 23]. Finally, we explore the range of 800 – 3000 Hz, which contains expected signals from binary neutron star mergers and postmerger physics [24, 25]. These phenomena are to date completely unexplored and could inform about exotic extreme states of matter [26].

Computationally simulating GW detectors – To compute the performance of a UIFO setup, we use `PyKat` [27], a Python interface for `Finesse`. `Finesse` (*Frequency domain INterfErometer Simulation SoftwarE*) is an open-source interferometer simulation program, with a main focus on GW physics [28]. `Finesse` computes the strain sensitivity over a frequency range of the GW of an experimental setup, such as those in Fig. 1. To computationally optimize the quality of an experimental detector design, we maximize the sensitivity while satisfying physical constraints for the parameters (such as maximal mirror reflectivity) and global constraints (such as maximal laser power that goes through an optical element). We compute the strain sensitivity, defined as the ratio between the optical response and the readout noise, at 100 discrete steps of the target frequency range.

`Urania`: A parallelized hybrid local-global optimizer for scientific discovery – Our goal of finding new GW detectors is translated into an optimization of a loss function that maximizes the detector sensitivity with experimentally feasible parameters and overall detector behavior. We develop `Urania`[1], a highly parallelized hybrid local-global optimization algorithm, sketched in Fig. 2A. It starts from a pool of 1000s of initial conditions of the UIFO, which are either entirely random initializations or augmented with solutions from different frequency ranges. `Urania` starts 1000 parallel local optimizations that minimize the objective function using an adapted version of the BFGS algorithm [29, 30, 31, 32]. For each local optimization, `Urania` chooses a target from the pool according to a Boltzmann distribution, which weights better-performing setups in the pool higher, and adds a small noise to escape local minima. When one of the local optimizations of `Urania` finds a better parameter setting for a setup in the pool, it replaces the old solution with the superior one. Upon convergence, `Urania` repeats and chooses a new target from the pool. In parallel, `Urania` simplifies solutions from the pool by probabilistically removing elements whose removal does not impact the overall sensitivity.

`Urania` can successfully navigate the complex search space, and discover in total 50 solutions that outperform the best-known human-designed topologies. Surprisingly, we observe that the solutions do not continuously improve, but go through phase transitions, with periods of neglectable improvements and periods where `Urania` identifies a superior strategy and exploits it to its fullest (see Fig.2B). In total, we spend roughly 1.5 million CPU-hours to identify the solutions. For a fair comparison

[1] In ancient Greek mythology, Urania is the muse of astronomy and stars.

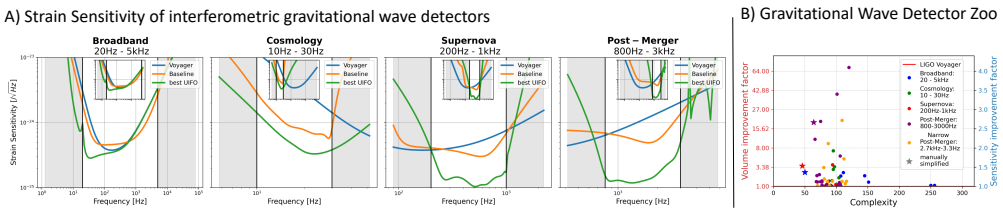

Figure 3: **Strain Sensitivity for various objectives**: A) Broadband, Cosmological Targets, Supernovæand ranges for the post-merger analysis of binary neutron star mergers. Blue: LIGO Voyager, Orange: LIGO Voyager with parameters optimized for the specific frequency range, Green: new UIFO solutions. Noise contributions involve quantum noise, laser frequency and intensity noises. B) Gravitational Wave Detector Zoo: We collect 50 experimental setups with improved sensitivity over the baseline, which is the parameter-optimized LIGO Voyager setup. Therefore, each solution not only has better parameters but also has a superior topology compared to LIGO Voyager.

with human-designed structures, we use a frequency-range-optimized version of the next-generation LIGO Voyager detector[9]. For that, the Voyager design in Fig. 4A is parametrized with more than 50 variables and extensively optimized with gradient-based methods. In that way, if a solution of `Urania` surpasses this baseline, we know that it needs to have not only better parameters of the optical elements for the same topology but an entirely new setup topology.

Results – We find a total of 50 UIFO configurations that outperform the optimized aLIGO baseline: 6 broadband solutions, 7 solutions for the cosmological window, 3 solutions for the supernova window, and the remaining 34 for analysing post-merger physics of neutron star mergers. In Fig. 3, we show the results of the best solutions in these four frequency regimes. For these four targets, we find a maximal sensitivity improvement of 4.2 compared to the optimized LIGO Voyager baseline (6.8 compared to the original LIGO Voyager), 2.2 (9.5), 4.0 (5.0) and 5.3 (9.0), respectively.

The improvements of the broadband solution lie predominantly in the low-frequency regime. This would improve the observation of heavy-mass black hole mergers. One of the key targets of LIGO is the observation of GW from supernovae. So far, no such event has been observed. The best solution we found improves the sensitivity on average by a factor of 1.6 compared to the optimized (baseline) Voyager detector. It thereby could increase the expected observation rate by a factor of 3.8. Finally, the expected frequency range of peaks of binary neutron star merger is currently outside of the most sensitive regime of LIGO. The average sensitivity in our best solution is improved by a factor of 4.1, potentially improving the rate by a dazzling factor of 68.7. In the appendix we investigate several of the top-performing solutions discovered by `Urania` to understand the underlying strategies that were used to go beyond human-designed detector ideas [33, 34].

Outlook – We demonstrate how large-scale digital exploration can discover new superior quantum-enhanced hardware for fundamental physics research. Going beyond the currently explored search space, for instance by adding quantum technologies [6, 35, 36] could lead to even further exciting and surprising solutions. While our solutions satisfy important experimental constraints, details about controllability, thermal noise contributions, tolerance to noise and optical loss could be directly embedded into the optimization objectives, potentially by co-designing of cryo-systems and mechanical suspensions of mirrors.

The high computational expense, over 1 million CPU hours, is due to the costly physical simulator. Future research could focus on creating an auto-differentiable simulator, similar to those in neural network computations [37], or develop neural-network-based surrogate models to efficiently approximate the physical simulator. The applications of our methodologies go far beyond gravitational wave physics. Due to the generality of our computational framework and the underlying physics that is governed by 2nd-order differential equations, our technology can straightforwardly be expanded to a large number of other experimental domains, including (quantum-enhanced) optics, mechanics, electronics or hydraulic design, and arbitrary combinations thereof. This will allow for exciting new hardware designs for practical applications and in fundamental science, such as dark matter [10, 11], dark energy detectors[38], and quantum gravity probes[12, 39, 13]. Therefore, automatically designing fundamental physics experiments might open new ways to observe the universe.

References

[1] Albert Einstein. Näherungsweise integration der feldgleichungen der gravitation. *Sitzungsberichte der Königlich Preußischen Akademie der Wissenschaften*, pages 688–696, 1916.

[2] Benjamin P Abbott, Richard Abbott, TD Abbott, MR Abernathy, Fausto Acernese, Kendall Ackley, Carl Adams, Thomas Adams, Paolo Addesso, RX Adhikari, et al. Observation of gravitational waves from a binary black hole merger. *Physical Review Letters*, 116(6):061102, 2016.

[3] B. P. Abbott, R. Abbott, T. D. Abbott, F. Acernese, K. Ackley, C. Adams, T. Adams, P. Addesso, R. X. Adhikari, et al. Multi-messenger observations of a binary neutron star merger. *The Astrophysical Journal Letters*, 848(2):L12, 2017.

[4] Junaid Aasi, BP Abbott, Richard Abbott, Thomas Abbott, MR Abernathy, Kendall Ackley, Carl Adams, Thomas Adams, Paolo Addesso, RX Adhikari, et al. Advanced LIGO. *Classical and quantum gravity*, 32(7):074001, 2015.

[5] Denis Martynov, Haixing Miao, Huan Yang, Francisco Hernandez Vivanco, Eric Thrane, Rory Smith, Paul Lasky, William E. East, Rana Adhikari, Andreas Bauswein, Aidan Brooks, Yanbei Chen, Thomas Corbitt, Andreas Freise, Hartmut Grote, Yuri Levin, Chunnong Zhao, and Alberto Vecchio. Exploring the sensitivity of gravitational wave detectors to neutron star physics. *Phys. Rev. D*, 99:102004, May 2019.

[6] Haixing Miao, Huan Yang, Rana X Adhikari, and Yanbei Chen. Quantum limits of interferometer topologies for gravitational radiation detection. *Classical and Quantum Gravity*, 31(16):165010, 2014.

[7] Aaron Buikema, Craig Cahillane, GL Mansell, CD Blair, Robert Abbott, C Adams, RX Adhikari, A Ananyeva, S Appert, K Arai, et al. Sensitivity and performance of the advanced ligo detectors in the third observing run. *Physical Review D*, 102(6):062003, 2020.

[8] Lisa Barsotti, Lee McCuller, Matthew Evans, and Peter Fritschel. The A+ design curve. *LIGO Document*, 1800042:2018, 2018.

[9] Rana X Adhikari, Koji Arai, AF Brooks, C Wipf, O Aguiar, Paul Altin, B Barr, L Barsotti, R Bassiri, A Bell, et al. A cryogenic silicon interferometer for gravitational-wave detection. *Classical and Quantum Gravity*, 37(16):165003, 2020.

[10] Sander M Vermeulen, Philip Relton, Hartmut Grote, Vivien Raymond, Christoph Affeldt, Fabio Bergamin, Aparna Bisht, Marc Brinkmann, Karsten Danzmann, Suresh Doravari, et al. Direct limits for scalar field dark matter from a gravitational-wave detector. *Nature*, 600(7889):424–428, 2021.

[11] Evan Hall and Nancy Aggarwal. Advanced LIGO, LISA, and Cosmic Explorer as dark matter transducers. *arXiv:2210.17487*, 2022.

[12] Aaron Chou, Henry Glass, H Richard Gustafson, Craig Hogan, Brittany L Kamai, Ohkyung Kwon, Robert Lanza, Lee McCuller, Stephan S Meyer, Jonathan Richardson, et al. The Holometer: an instrument to probe Planckian quantum geometry. *Classical and Quantum Gravity*, 34(6):065005, 2017.

[13] Dongjun Li, Vincent SH Lee, Yanbei Chen, and Kathryn M Zurek. Interferometer response to geontropic fluctuations. *Physical Review D*, 107(2):024002, 2023.

[14] Mario Krenn, Mehul Malik, Robert Fickler, Radek Lapkiewicz, and Anton Zeilinger. Automated search for new quantum experiments. *Physical review letters*, 116(9):090405, 2016.

[15] Mario Krenn, Manuel Erhard, and Anton Zeilinger. Computer-inspired quantum experiments. *Nature Reviews Physics*, 2(11):649–661, 2020.

[16] Mario Krenn, Jakob S Kottmann, Nora Tischler, and Alán Aspuru-Guzik. Conceptual understanding through efficient automated design of quantum optical experiments. *Physical Review X*, 11(3):031044, 2021.

[17] Kurt Hornik. Approximation capabilities of multilayer feedforward networks. *Neural networks*, 4(2):251–257, 1991.

[18] Tilman Hartwig, Marta Volonteri, Volker Bromm, Ralf S Klessen, Enrico Barausse, Mattis Magg, and Athena Stacy. Gravitational waves from the remnants of the first stars. *Monthly Notices of the Royal Astronomical Society: Letters*, 460(1):L74–L78, 2016.

[19] Marcelle Soares-Santos, A Palmese, W Hartley, James Annis, J Garcia-Bellido, O Lahav, Z Doctor, M Fishbach, DE Holz, H Lin, et al. First measurement of the Hubble constant from a dark standard siren using the dark energy survey galaxies and the LIGO/Virgo binary–black-hole merger GW170814. *The Astrophysical Journal Letters*, 876(1):L7, 2019.

[20] Christian D Ott. The gravitational-wave signature of core-collapse supernovae. *Classical and Quantum Gravity*, 26(6):063001, 2009.

[21] H Andresen, E Müller, H-Th Janka, A Summa, K Gill, and M Zanolin. Gravitational waves from 3D core-collapse supernova models: The impact of moderate progenitor rotation. *Monthly Notices of the Royal Astronomical Society*, 486(2):2238–2253, 2019.

[22] VP Utrobin, A Wongwathanarat, H-Th Janka, E Müller, T Ertl, A Menon, and A Heger. Supernova 1987A: 3D mixing and light curves for explosion models based on binary-merger progenitors. *The Astrophysical Journal*, 914(1):4, 2021.

[23] David Vartanyan, Adam Burrows, Tianshu Wang, Matthew SB Coleman, and Christopher J White. Gravitational-wave signature of core-collapse supernovae. *Physical Review D*, 107(10):103015, 2023.

[24] Sebastiano Bernuzzi, Tim Dietrich, and Alessandro Nagar. Modeling the complete gravitational wave spectrum of neutron star mergers. *Physical Review Letters*, 115(9):091101, 2015.

[25] Teng Zhang, Huan Yang, Denis Martynov, Patricia Schmidt, and Haixing Miao. Gravitational-wave detector for postmerger neutron stars: Beyond the quantum loss limit of the fabry-perot-michelson interferometer. *Physical Review X*, 13(2):021019, 2023.

[26] M. Agathos, J. Meidam, W. Del Pozzo, T. G. F. Li, M. Tompitak, J. Veitch, S. Vitale, and C. Van Den Broeck. Constraining the neutron star equation of state with gravitational wave signals from coalescing binary neutron stars. *Phys. Rev. D*, 92:023012, Jul 2015.

[27] Daniel D. Brown, Philip Jones, Samuel Rowlinson, Sean Leavey, Anna C. Green, Daniel Töyrä, and Andreas Freise. `PYKAT`: Python package for modelling precision optical interferometers. *SoftwareX*, 12:100613, 2020.

[28] Daniel David Brown and Andreas Freise. Finesse, May 2014. The software and source code is available at `http://www.gwoptics.org/finesse`.

[29] Charles George Broyden. The convergence of a class of double-rank minimization algorithms 1. general considerations. *IMA Journal of Applied Mathematics*, 6(1):76–90, 1970.

[30] Roger Fletcher. A new approach to variable metric algorithms. *The computer journal*, 13(3):317–322, 1970.

[31] Donald Goldfarb. A family of variable-metric methods derived by variational means. *Mathematics of computation*, 24(109):23–26, 1970.

[32] David F Shanno. Conditioning of quasi-newton methods for function minimization. *Mathematics of computation*, 24(111):647–656, 1970.

[33] Ted Chiang. Catching crumbs from the table. *Nature*, 405(6786):517–517, 2000.

[34] Mario Krenn, Robert Pollice, Si Yue Guo, Matteo Aldeghi, Alba Cervera-Lierta, Pascal Friederich, Gabriel dos Passos Gomes, Florian Häse, Adrian Jinich, AkshatKumar Nigam, et al. On scientific understanding with artificial intelligence. *Nature Reviews Physics*, 4(12):761–769, 2022.

[35] Roman Schnabel, Nergis Mavalvala, David E McClelland, and Ping K Lam. Quantum metrology for gravitational wave astronomy. *Nature communications*, 1(1):121, 2010.

[36] Quntao Zhuang, John Preskill, and Liang Jiang. Distributed quantum sensing enhanced by continuous-variable error correction. *New Journal of Physics*, 22(2):022001, 2020.

[37] James Bradbury, Roy Frostig, Peter Hawkins, Matthew James Johnson, Chris Leary, Dougal Maclaurin, George Necula, Adam Paszke, Jake VanderPlas, Skye Wanderman-Milne, and Qiao Zhang. JAX: composable transformations of Python+NumPy programs. 2018.

[38] Paul Hamilton, Matt Jaffe, Philipp Haslinger, Quinn Simmons, Holger Müller, and Justin Khoury. Atom-interferometry constraints on dark energy. *Science*, 349(6250):849–851, 2015.

[39] Sander M Vermeulen, Lorenzo Aiello, Aldo Ejlli, William L Griffiths, Alasdair L James, Katherine L Dooley, and Hartmut Grote. An experiment for observing quantum gravity phenomena using twin table-top 3d interferometers. *Classical and Quantum Gravity*, 38(8):085008, 2021.

[40] Alessandra Buonanno and Yanbei Chen. Signal recycled laser-interferometer gravitational-wave detectors as optical springs. *Phys. Rev. D*, 65:042001, Jan 2002.

[41] Samuel Schulz, Yehonathan Drori, Christopher Wipf, and Rana X Adhikari. Optical refrigeration for an optomechanical amplifier. *arXiv:2212.01442*, 2022.

[42] Michael A. Page, Maxim Goryachev, Haixing Miao, Yanbei Chen, Yiqiu Ma, David Mason, Massimiliano Rossi, Carl D. Blair, Li Ju, David G. Blair, Albert Schliesser, Michael E. Tobar, and Chunnong Zhao. Gravitational wave detectors with broadband high frequency sensitivity. *Communications Physics*, 4(1):27, Feb 2021.

[43] H. J. Kimble, Yuri Levin, Andrey B. Matsko, Kip S. Thorne, and Sergey P. Vyatchanin. Conversion of conventional gravitational-wave interferometers into quantum nondemolition interferometers by modifying their input and/or output optics. *Phys. Rev. D*, 65:022002, Dec 2001.

[44] V.B. Braginsky and F.Ya. Khalili. Low noise rigidity in quantum measurements. *Physics Letters A*, 257(5):241–246, 1999.

A Appendix

Physics of discovered solutions

We investigate several of the top-performing solutions discovered by `Urania` to understand the underlying strategies that were used to go beyond human-designed detector ideas [33, 34]. The implementation of most of the solutions do not require severe changes to the existing LIGO sites' infrastructure or the construction of kilometer-scale vacuum tubes, thus are candidates for potential future detector upgrades.

An unusual side-pumped L-shape GW transducer – Most solutions, like those in Fig.4A or B, diverges from the standard Michelson interferometer-based LIGO topology. These setups employs two lasers pumping the arms from their high reflectivity sides, enabling lower-power lasers (e.g., two $36\,\mathrm{W}$ lasers in the broadband solution versus a single $152\,\mathrm{W}$ laser in LIGO Voyager).

Pondermotive squeezing – To boost quantum-limited sensitivity, `Urania` finds numerous solutions that incorporate pondermotive squeezing and amplification in the arms or external lightweight cavities [40]. Experimentally, the high circulating power in the external optomechanical cavities and the small mirror masses present challenges for radiatively-cooled mirrors in cryogenic interferometers. Alternative methods such as optical refrigeration of mirrors [41] or the use of mechanical resonators [42] instead of free masses could lift these limitations.

The Physics of the Broadband Solution – Fig. 4A shows details for a broadband GW detector. The GW signal exiting the open port of the $4.8\,\%$ corner beamsplitter is routed through the Faraday isolators and filtered by a $3\,\mathrm{km}$ filter cavity. A $10\,\mathrm{dB}$ squeezed vacuum is injected into the dark port. The filter cavity allows utilization of the pondermotive squeezing generated in the arms to enhance the low-frequency sensitivity of the solution similar to a variational readout scheme proposed in [43]. This interpretation is strengthened by Fig. 4A **ii** and **iii**, showing that the quantum noise does not diverge as frequency tends to zero and that the response vanishes for zero frequency, respectively, and the highly suppressed coupling of amplitude fluctuations to the readout at all frequencies. Surprisingly, unlike the original variational readout scheme, a small part of the light in the filter cavity is routed back into the interferometer. This creates a weak optical spring resonance [40] that enhances the quantum-limited sensitivity at $30\,\mathrm{Hz}$ by a factor of 1.4 compared with the case where the filter is completely sealed.

The Physics of the Supernova Solution – Fig. 4B shows the optical layout and performance of the solution optimized for supernova GW signals. The GW transducer's topology is the same as the one in the broadband solution. However, in this case, the outputs of the transducer are used as inputs to a ring cavity that encompasses a $17\,\mathrm{m}$ linear cavity formed by $10\,\mathrm{g}$ mirrors which enhances greatly the optomechanical effects. Since the optomechanical cavity is housed inside a cavity that feeds the signal back into the interferometer, it acts as an optical spring [40]. In addition to the optomechanical cavity, the ring cavity also contains a $700\,\mathrm{m}$ long filter cavity that aligns the frequency-dependant vacuum squeezing angle with the signal phase. Figs. 4B **ii** and **iii** show the quantum noise and the optical response respectively. The dashed green lines in the figures show the noise and the response without radiation pressure effects. Remarkably, in the presence of radiation pressure, the GW signal gets amplified by 3 orders of magnitude, while at the same time, the quantum noise is amplified by a small amount. This is a new generalization of optical springs, with special cases applied to the standard aLIGO topology before [40, 44].

The Physics of the Postmerger Solution – Fig. 4C shows the optical layout and performance of the solution optimized for postmerger signal of a binary neutron star coalescence. This setup is the most unintuitive of the three presented here. Instead of pumping the interferometer directly through the arm cavity, one of the lasers pumps it from the end recycling mirror. Similarly to the supernova solution, this solution uses an external short $10\,\mathrm{g}$ cavity and a $100\,\mathrm{m}$ filter cavity for resonantly enhancing the signal at the target frequency band.

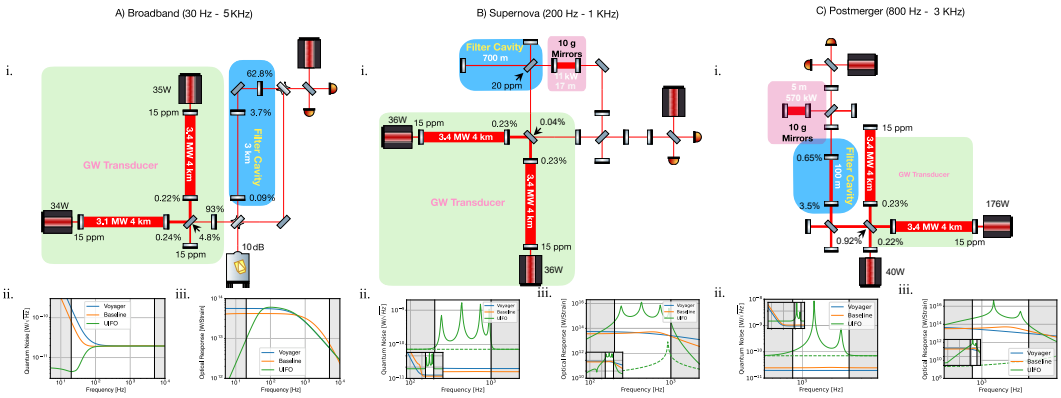

Figure 4: **Conceptualized UIFOs:** For each of the 3 simplified UIFOs **i.** Optical layout diagram illustrating the solution, highlighting essential optical parameters. The percentage alongside the mirrors and beamsplitters indicate their power transmission coefficients, while the values (in white) in or near the spaces denote their length and the optical power circulating inside them. Optical detunings are omitted for clarity. Spaces with no length notation can be arbitrarily short. As a consequence, many optical elements can be grouped together on suspended platforms, thus simplifying the control over these elements. Light traveling against the direction of the arrow of the Faraday isolator is transmitted, whereas light traveling in the same direction as the arrow is reflected. **ii.** Quantum noise of the UIFO solution (green), the baseline (orange), and Voyager (blue). **iii.** Optical response of the solution (orange), the baseline (green), and Voyager (blue). In Figures B) and C), the dashed green line shows the computed curve for the UIFO without radiation pressure demonstrating the dramatic effect of optomechanical coupling on the UIFO's performence. The frequency axes in B) and C) span the targets' frequency ranges. Insets show the curves in the broad frequency range.